VOL. 18, NO. 17, SEPTEMBER 2023 ISSN 1819-6608
ARPN Journal of Engineering and Applied Sciences

www.arpnjournals.com

DOUBLY SELECTIVE WITH EXPECTATION MAXIMIZATION BASED MASSIVE-MIMO-NON-ORTHOGONAL MULTIPLE ACCESS SYSTEMS

V. Satya Kumar Kudipudi and S. Neeraja
Department of Electrical Electronics and Communication Engineering, GITAM (Deemed to be University), Visakhapatnam, Andhra Pradesh, India
E-Mail: k.v.satyakumar@gmail.com

ABSTRACT

The Long-Term Evaluation (LTE) based Fourth Generation (4G) and Fifth Generation (5G) communications require higher data rates to satisfy the requirements of user equipment. However, it is a difficult task for conventional Multiple Input Multiple Output (MIMO) systems to deliver the highest throughput and data rates to end users. Additionally, an increase in data rates led to increased power consumption, which decreased spectrum efficiency and energy efficiency. Therefore, this paper focuses on the implementation of the Doubly Selective with Expectation Maximization (DSEM) channel estimation method for Massive-MIMO based Non-Orthogonal Multiple Access (NOMA) systems. Here, the DSEM scheme divides the channel into expectation and maximization vectors based on antenna diversity. Further, time sample and frequency band base dual channel analysis are performed to maintain the synchronization in the receiver. The simulations conducted using MatlabR2018a show that base station (BS) capacity, user equipment capacity, uplink (UL)-Spectrum Efficiency (SE), and downlink (DL)-SE performance measures are improved in Massive-MIMO-NOMA systems using DSEM channel estimation and shows the superior performance than state of art approaches.

Keywords: massive MIMO systems, NOMA, capacity, spectrum efficiency, downlink SE, expectation-maximization based doubly selective.

Manuscript Received 29 June 2023; Revised 24 October 2023; Published 8 November 2023

1. INTRODUCTION

The 4G and 5G cellular concepts [1], along with digital technology, enabled commercial wireless networks and transformed a mere cellular phone, meant for a voice call into a pillar of social communication. Ever since the arrival of mobile data, researchers [2] have been trying to achieve higher data rates and capacity. The focus has been a seamless user experience from the perspective of multimedia streaming [3]. The need for a packet-switched, flat architecture-based system targeting anytime, anywhere connectivity with higher data rates and SE gave birth to the 5G cellular wireless [4]. The age of 5G brings the Industrial Revolution, a convergence of the physical, digital, and biological worlds. The integration and innovation across distinct, siloed fields have enabled an entirely new set of applications with new parameters defining the Quality of Service (QoS) [5]. The rapid growth in data and devices is changing how smart applications are built to deliver an exceptional experience to users. Traffic per 5G connection will get tripled by 2023 as compared to a 4G connection [6]. Figure-1 demonstrates the requirements for enabling 5G services.

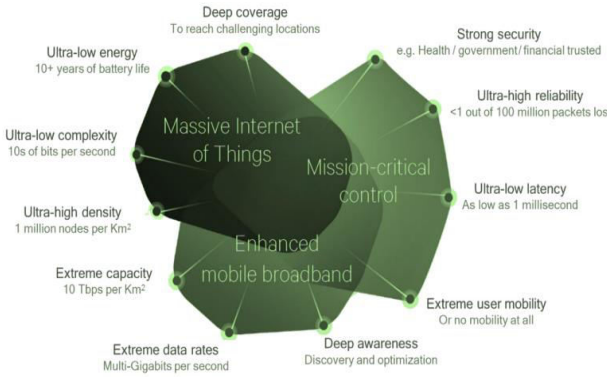

Figure-1. 5G Requirements.

Immersive applications based on AR/VR technology [7] along with Holographic content and multi-sense haptic communication services shall enable new exciting use cases varying from entertainment to life-impacting, e.g., telesurgery. These 5G communication requirements were satisfied by implementing the advanced Massive MIMO system [8], NOMA systems [9], and hybrid systems. The Massive-MIMO-NOMA is a hybrid system, which gives the prominent solution than other systems.

In the Massive-MIMO-NOMA systems [10], various techniques are developed for reducing the pilot contamination effect. Intra-cell points reuse methods by controlling spatially linked Rician fading channels are utilized to decrease the pilot contamination effect. Another method is the joint plan of the channel estimation and a

pilot assignment approach through utilizing the channel sparsity to decrease the pilot contamination [11]. Furthermore, the pilot allocation method, like the Graph coloring algorithm is introduced to reduce the pilot contamination. Various channel estimation techniques [12] are developed for managing pilot contamination. If the multipath components of the channel vector have imperfect angular speed, then, the coordination of pilot transmission in adjacent cells is possible. On the other hand, the channel vectors should be identified at the BS for efficiently dividing the co-pilot users and covariance information [13]. A priori statistical knowledge is utilized for reusing the pilots in a similar cell, which reduces the pilot dimension overhead. The following are the main contributions of this work:

The Massive-MIMO-NOMA systems are implemented to improve spectrum efficiency and energy efficiency in cellular networks.

Implementation of DSEM channel estimation for improved channel matrix identification with reduced errors.

Simulations are conducted over 250 BS antennas and 100 UEs with effective channel properties.

The remaining portions manuscript are structured as follows: section 2 deals with the survey of various Massive-MIMO-NOMA systems with diverse channel estimation models. Section 3 deals with the detailed analysis of the proposed DSEM channel estimation baaed Massive-MIMO-NOMA system. The simulation output produced by the MatlabR2018a software is covered in Section 4. The potential future scope is discussed in Section 5 of this paper.

2. RELATED WORK

In this section, this paper considers the massive MIMO system's downlink while assuming that the BS has incomplete CSI. Sum rate maximizing hybrid precoders are based on partial CSI, which was obtained in [14] for broadband mmWave communication systems. A fully connected architecture in which the output of each RF chain is sent to each antenna by phase shifters is employed for a multiuser mmWave MISO system. The above problem is converted into a sparse digital Non-deterministic Polynomial-Hard problem [15] and two solutions based on norm relaxation and successive convex approximation are proposed. Further, the complexity of using a hybrid precoding design is reduced by using subcarrier grouping and an equal power allocation scheme. A limited feedback design [16] utilizing the SVD of an effective channel matrix is proposed. Also, Low rank and Givens Transform result in a reduction of feedback overheads.

In [17] authors compared sub-connected and fully connected Successive Sub-Array Activation (SSAA) precoding architectures for Massive-MIMO-NOMA environment. In particular, analysis of SE for sub-connected and fully connected system structures using the channel correlation-based codebook is performed. The proposed approach outperforms the random vector quantization codebook design when used with sub-connected structures. In [18] authors achieved optimal capacity with Wavelet Pulse Shaping (WPS) based channel estimation. The proposed WPS precoding technique is based on selective eigenvalue information and limited feedback and analyzed performance using a combination of codebook-based and discrete quantized feedback [19]. The proposed scheme jointly makes use of individual quantized and codebook-based feedback. The optimal feedback bit allocation is determined and used in the abovementioned feedback methods to minimize the throughput loss with the feedback link capacity constraint. In [20] authors focused on the improvement of limited feedback hybrid beamforming systems achieved by the Beam selection method. The joint channel estimation problem [21] is independently solved by utilizing beam selection with Group Successive Interference Cancellation (GSIC) channel estimation. The GSIC selection is based upon the feedback of codebook evaluation for analog precoder and zero forcing in digital precoding. The users evaluate the codebook after receiving channel state information and then feedback on the values and/or beam index corresponding to the maximum SNR to the BS for analog precoder selection. In [22] authors proposed the usage of the baseband precoding matrix obtained from CV-BLAST implementation to modify the RF precoder. A modified analog precoding matrix is then used to update the entries of the baseband precoding matrix [23]. This refinement procedure goes on until the variance among two successive distortion values falls lower than the threshold. In the limited feedback case, the Grassmannian codebook is used to quantize the baseband precoder, and the K-means clustering algorithm is used to quantize the RF precoder.

In [24] authors designed the beamforming matrix based using LS and MMSE methods. Two schemes based on one and two-stage feedback in conjunction with statistical CSIT and adaptive codebook are evaluated over different conditions [25]. Analog beam former is designed based on one-stage feedback which utilizes all feedback resources and the multiuser interference is mitigated by using the statistical CSIT [26]. In two-stage schemes, the second stage is introduced for effective quantization of the channel resulting in improved interference mitigation as compared to the stage scheme. Further, to improve their performance, rate splitting is proposed. In [27] authors implemented another variant of precoding called frequency selective hybrid precoding is analyzed for limited feedback systems. The authors propose an efficient RF and baseband codebook design for hybrid precoded mmWave systems [28]. The authors also demonstrated an algorithm for downlink multiuser hybrid beamforming codebook construction followed by the derivation of a hybrid precoder based on the Gram-Schmidt method for frequency selective channels. It is shown that feeding back only the indices of the RF precoder would be enough for maximizing mutual information for the cases when the count of the data stream is the same as RF chains. In addition, it is also shown that the sequential design of hybrid precoders performs similarly to iteratively updated jointly designed precoders.

In [29] authors improved the SE by using Gradual Resource Allocation (GRA) channel estimation techniques on the receiver side. They derived tight bounds on achievable rate over a Massive MIMO downlink with partial CSI by accounting quantization effects. The authors derive closed-form expressions demonstrating the superior performance of analog precoding over hybrid precoding for zero forcing and maximal-ratio-transmission w.r.t. several feedback bits, count of users, and the SNR over mmWave as well as the Rician channel. In [30] authors developed a Deep Neural Network (DNN) based codebook for multiuser hybrid precoded systems to reduce the beam training overheads. The proposed scheme performs similarly to traditional schemes with lesser complexity and limited beam training. The channel subspace for implementing the outer-tier precoding using a high-dimensional quantized Grassmannian product is used. The proposed scheme overcomes the inefficiency of DFT codebooks associated with increasing codebook sizes by varying the quantization dimensions.

3. PROPOSED METHOD

The traditional antenna systems are unable to result in improved capacity needs for the user equipment, due to limitations of the technology. These days, more complex kinds of MIMO are being created; the approach that focuses mostly on multiuser is explored in our thesis. The proposed Massive-MIMO-NOMA system with DSEM channel estimate may be seen shown in Figure-2.

In this scenario, the signal that is received by each of the receivers is influenced by the signal that is sent by each of the transmitter antennas. For the purpose of modeling a channel, a narrow band with a flat fading channel will be studied, and expressions will be used in the frequency domain. The signal is portrayed when it is received by one antenna given as follows:

$$y_{f_o}^{r} = \sum_{t=1}^{N_t} y_{f_o}^{N_r} + W_k^r \quad (1)$$

In this context, t, r refers to the transmitter index and the receiver index, whereas f_o denotes the operating frequency. The time index was removed so that the notation could be made simpler. In addition, the numbers $N_t$and N_r refer to the number of transmitters and receivers that are a part of the system. In earlier works, the Massive-MIMO-NOMA channel was described on the premise that the fading model was flat. This is not the case with a wideband system, in which the channel responds somewhat differently to each section of the spectrum. Strong fades brought on by multipath, for example, might result in changes of more than 20 dB, which means that the model for the Massive-MIMO-NOMA capacity is no longer viable. This does produce a collection of distinct channels, and every single one of them satisfies the Massive-MIMO-NOMA criteria that were described before. Once all of the narrowband capabilities have been added together, the resulting capacity will be determined. A higher-level modulation may be used in a band if, as a matter of course, one sub-band has lower attenuation levels than the others do and a greater signal-to-noise ratio.

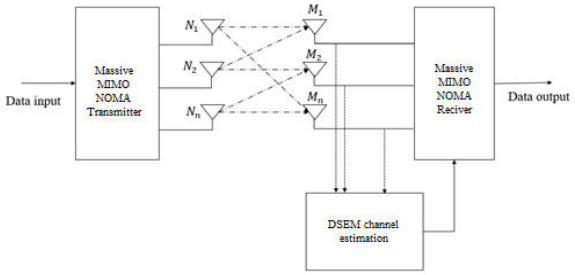

Figure-2. Massive-MIMO-NOMA with DSEM channel estimation.

Many wireless systems, such as DSL technologies, take advantage of the independence of the sub-bands by transmitting a distinct number of bits for each sub-band. This practice is common. It is necessary to have CSI present at the transmitter for this to be feasible. On the other hand, feedback information from the receiver cannot be delivered to the transmitter in uniform power allocation (UPA) channels any quicker than the temporal coherence of the channel. Because of this, DSEM channel estimation makes use of UPA in conjunction with the same kind of modulation for each of the sub-bands. The intricacy of the wireless gadget, on the other hand, ought to be low, as must its power consumption. Because of this, building algorithms and designs for the mobile receiver presents several issues. Emerging wireless systems have needs that aren't very complicated if any at all. In addition, the appropriateness of various algorithms for wireless systems is determined by considering a significant number of system characteristics. Channel estimation and interference mitigation methods, as well as the requirements for implementing them, are the primary focuses of this study. In the area of wireless communications, the Massive-MIMO-NOMA technology has garnered a lot of interest.

3.1 System Model

The subproblem of sparse channel estimation related to wireless communications is considered here. In the fundamental system model, the desired signal is transmitted through linear channels with AWGN. The governing input-output equation is.

$$y = Hs + w \quad (2)$$

where y represents the received signals, $H \in C\ mxm$ gives the system matrix, s represents the targeted signal vector, and 'w' refers noise ($w \sim CN(0, \sigma^2)$). For such cases the targeted vector s is considered sparse, implying that the part of non-zero entries in s is very much smaller than its dimension. It is crucial to remember that even when the required vector is not sparse, a suitable transformation can be used to approximate the desired vector or convert it to a sparse vector. When the value of non-zero elements is small, an approximately sparse

vector can be determined by neglecting small nonzero elements. By correctly selecting basis $\psi = [\psi_1 \ldots . \psi_n]$, the input vector can become

$$S = \sum_{i=1}^{n} x_i * \psi_x \quad (3)$$

Here, ψ_x represents S in the frequency domain. Through proper ideology of basis, converting the original non-sparse vector S into the sparse vector ψ_x. The new representation does not alter the system model eventually and results in superior capacity levels. These properties make Massive-MIMO-NOMA an attractive research area in the field of communication.

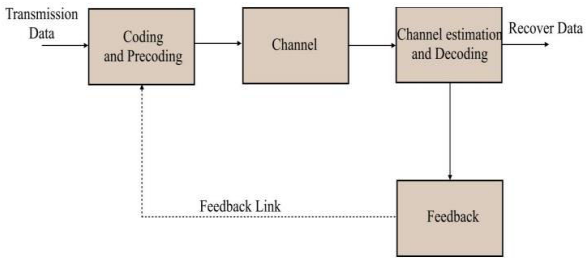

Figure-3. DSEM channel estimation-based receiver feedback model.

Due to its amplitude, phase, and wavelength, a wireless communication channel has significant random ratings. Measurement of the channels and recognition of reception as a receiver's decisive components is essential for wireless communications. Channel estimation technique: Communication systems usually complete channel estimation at the receiver, and the precision of the estimation has a significant effect on overall device performance. Channel prediction algorithms can be classified into two types based on the transmitting signal: frequency domain and time domain. They can be known as reference signal estimates, blind estimates, or half-blind estimates depending upon whether prior information is required. Usually, the pilot sequence provides a more convincing approximation result based on the reference signal. To achieve high spectral efficiencies for blind and half-blind estimates, a brief sequence is needed. Nevertheless, the associated drawbacks are poor precision of estimates, significant uncertainty in the process, and estimated non-convergence issues. To increase the bandwidth of the channel, the transmitter and receiver need the CSI with DSEM channel estimation. As seen in Figure-3, the DSEM channel estimation of the transmitter is recovered and transmitted through the receiver. In the practical application of Massive-MIMO-NOMA technology, reception identification of the Massive-MIMO-NOMA communication device is critical. There are two types of signal detection algorithms: linear and nonlinear. The obtained signal will reconstruct the initially transmitted signal entirely through linear operations in linear detection.

3.2 DSEM Channel Estimation

The arrival of 4G cellular connections, also known as LTE, which provides downlink rates in the region of 100-150 Mbps, has enabled this change in behavior (3GPP R1-162199, 2016). Live High Definition (HD) video streaming and online gaming over the air interface are examples of 4G uses. As the deployment of 4G networks throughout the world nears completion, the mobile communication industry has moved on to the development and implementation of 5G networks. Clients may face a variety of Doppler shifts, recurrence balances, temporal counterbalances, and so on, and maintaining symmetry between the subcarriers may be impossible without energy-draining and asset-requesting techniques.

Furthermore, owing to the high side-projection levels of its subcarriers, using non-touching range lumps through bearer accumulation for future high information rate applications is not possible in the uplink with Massive-MIMO-NOMA. Furthermore, massive monitor groups are necessary between adjoining recurrence channels to keep a strategic distance from impedance, lowering the unearthly efficacy of Massive-MIMO-NOMA. Thus, the proposed DSEM channel estimation effectively enhances the work efficiency of conventional Massive-MIMO-NOMA systems.

Figure-4 presents the architecture of DSEM channel estimation with a channel impulse response matrix. Here, KF is the kappa factor, h is time-based pilots, m is frequency-based pilots, a_{p_n} = error-free output, y_{p_n} is the received data, p is the prediction value of channel matrix h, e is estimated value of h, n-1 represents the previous samples, $r_n(k)$represents the received pilot with samples k. Table-1 presents the proposed DSEM channel estimation algorithm.

The time and frequency-dependent pilots are generated by the doubly selective channel estimation using the EM operation, and the time-based pilot symbols are applied using the expectation operation and the frequency-based pilot symbols are applied using the maximization operation. The updated channel matrix with highly accurate pilots would be the product of this EM-step. The data will be perfectly adjusted by using three steps to mitigate the error which is 1. Initialization Path, 2. Error detection, and 3. Final Error Correction.

Initialization path

This process starts from KF Correction to Z^{-1} from Z inverse transformation to Channel and MSE Prediction method to KF Correction, this path is used to update the pilots at the receiver side every time.

Error detection

This error detection path starts from KF correction to one Tap Equalizer and compares with EM-block, at last, it connects to KF correction. In this path, the received pilots are compared with the transmitted pilots and result in error-free data output. If the errors are still present, further it is performed by the final error correction path.

Final error correction

The final path starts from KF Correction to One Tap Equalizer to EM-block and passes through, Channel and MSE Prediction to KF Correction. In this path, if a multiple number of errors are present then new channel prediction values are generated by the updated channel impulse matrix. At last, all types of errors will be suppressed by using the updated values, and at each time and frequency sample, the data is adjusted perfectly.

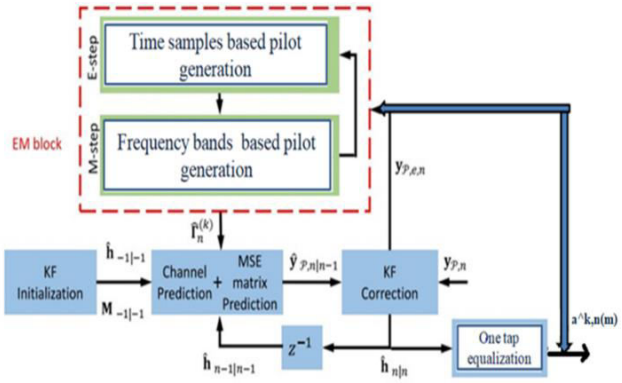

Figure-4. Block diagram of DSEM channel estimation.

Table-1. DSEM channel estimation algorithm.

Input: Received signal ($Y_{P,n}$), KF coefficients. **Output:** Error-free output data ($\hat{Y}_{p,n\|n-1}$)
Step 1: Apply the received channel signal to KF correction, here all the AWGN noise levels are identified.
Step 2: Initialize the KFs, which are used to generate the channel matrix ($\hat{h}_{-1\|-1}$) with fundamental error correction properties.
Step 3: Then the KF correction outcomes are applied to Z^{-1} block, which is considered as the error correction initialization.
Step 4: The erroneous channel response ($\hat{h}_{n-1\|n-1}$) is applied to channel prediction along with maximum MSE prediction operation.
Step 5: During the error detection process, the channel matrix ($\hat{h}_{n\|n}$) is applied to the one-tap equalizer. Here, the weight updating matrix ($\hat{a}_{n\|m}$) is generated, which can be used to equalize the channel coefficients based on error probability levels.
Step 6: During the final error correction process, the weight updating matrix ($\hat{a}_{n\|m}$) and KF error detected coefficients ($Y_{P,e,n}$) are applied to the EM block.
Step 7: E-step is used to generate the synchronized received data based on the time samples, which is used to expertise the time-based pilots with high priority levels.
Step 8: M-step is used to generate the synchronized frequency domain data based on the frequency samples, which is used to maximize the frequency dominant pilots with accurate priority levels.
Step 9: Both, the EM steps are used to synchronize the received data generate the new channel response matrix (r_n^k), and apply it to channel prediction.
Step 10: Final channel prediction is performed with reduced MSE values is performed based on previous channel coefficients such as $\hat{h}_{-1\|-1}$, $\hat{h}_{n-1\|n-1}$, and r_n^k, which generates the final output as error-free output data ($\hat{Y}_{p,n\|n-1}$).
Step 11: The process of initialization, basic error detection, and final error correction paths are iterated through the EM block and channel prediction generates the efficient channel vectors each time with maximum data rate and success rate.

4. RESULTS AND DISCUSSIONS

This section provides a thorough analysis of simulation results that were carried out using MatlabR2018a. Furthermore, the efficacy of the proposed approach is compared with state of art approaches using the same environment.

4.1 Simulation Parameters

The simulation parameters are displayed in Table-2. A Gaussian compound distribution with a zero mean and a unit variance is produced by the channel's non-zero coefficients. A radio propagation anomaly brought on by the partial cancellation of an RF signal alone is modeled stochastically by rician fading. The signal exhibits multipath interference because it travels along several separate pathways to reach the receiver, at least one of which is shifting. The partial cancellation of an RF signal by itself (lengthening or shortening) results in Rician fading. Rician fading occurs when one of the paths is frequently a signal traveling in a line-of-sight or some strong reflection signals. It is possible to consider the Rician distribution as the distinguishing characteristic of the amplitude gain in Rician fading.

Table-2. Simulation parameters.

Parameters	Value
Number of BS Antennas	250
Kappa Values BS	[0, 0.05^2, 0.15^2]
Kappa Values UE	[0, 0.05^2, 0.15^2]
Number of UEs	1000
Channel Type	Rician
Signal-to-Noise Ratio Range	0-20dB
Traffic Portion	0.45

4.2 Performance Evaluation

Figure-5 represents the proposed DSEM channel estimation-based downlink SE performance comparison with conventional approaches such as SSAA [17], WPS [18], GSIC [21], and GRA [29] in Massive MIMO-NOMA environment for 250 antennas. The proposed DSEM channel estimation resulted in 6.2 Mbps/Hz, whereas conventional WPS [18] resulted in 4.23 Mbps/Hz, GSIC [21] resulted in 3.42 Mbps/Hz, SSAA [17] resulted in 2.4 Mbps/Hz, and GRA [29] resulted in 2.1 Mbps/Hz at N=250.

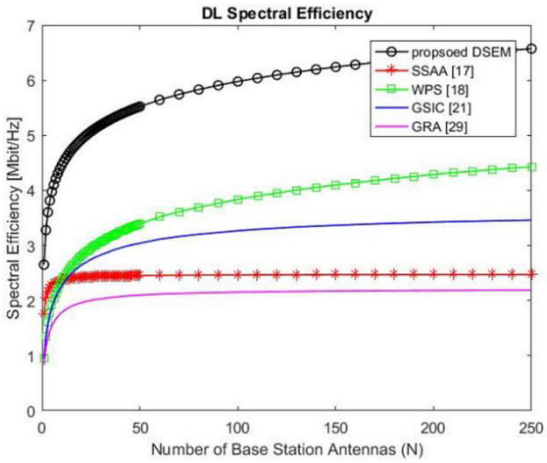

Figure-5. Downlink SE performance estimation.

Figure-6 represents the proposed DSEM channel estimation-based uplink SE performance comparison with conventional approaches such as SSAA [17], WPS [18], GSIC [21], and GRA [29] in a Massive MIMO environment for 250 antennas. The proposed DSEM channel estimation resulted in 3.6 Mbps/Hz, whereas conventional WPS [18] resulted in 2.7 Mbps/Hz, GSIC [21] resulted in 2.6 Mbps/Hz, SSAA [17] resulted in 2.3 Mbps/Hz, and GRA [29] resulted in 2 Mbps/Hz at N=250.

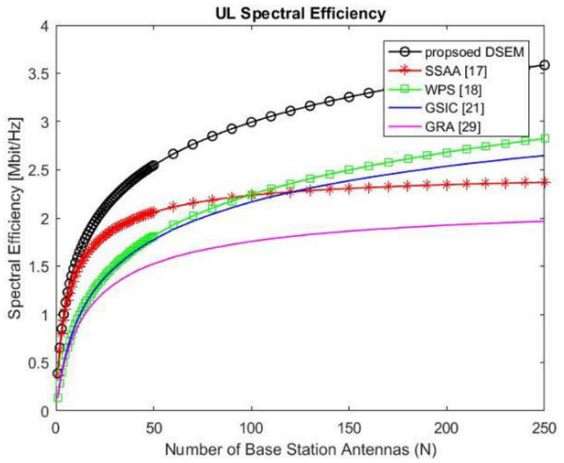

Figure-6. Uplink SE performance estimation.

Figure-7 represents the capacity performance of Massive-MIMO-NOMA systems for multiple numbers of UEs. The proposed DSEM channel estimation algorithm performed superior to SSAA [17], GSIC [21], GRA [29], and WPS [18] algorithms. The proposed DSEM channel estimation resulted in 3.8 Mbps/Hz, whereas conventional SSAA [17] resulted in 3.5 Mbps/Hz, GSIC [21] resulted in 3.4Mbps/Hz, WPS [18] resulted in 3.45 Mbps/Hz, and GRA [29] resulted in 3.1 Mbps/Hz for 1000 number of UEs. Here, the total 1000 UEs are considered, which shows that the proposed DSEM channel estimation resulted in an improvement of capacity.

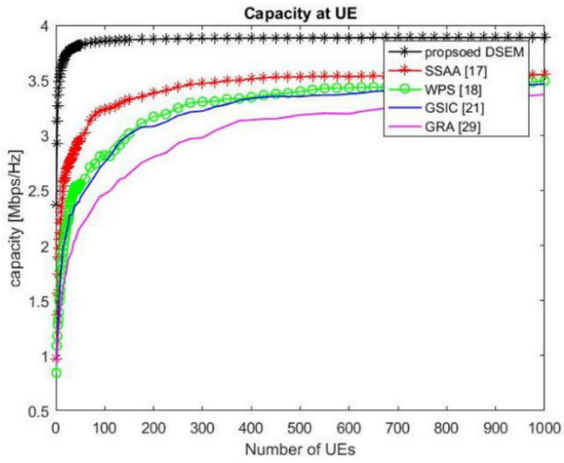

Figure-7. UE capacity performance estimation

Figure-8 represents the capacity estimation of Massive-MIMO systems for 250 BSs. The proposed DSEM channel estimation algorithm performed superior to SSAA [17], GSIC [21], WPS [18], and GRA [29] algorithms. The proposed DSEM channel estimation achieved 6Mbps/Hz of capacity, whereas conventional methods achieved 3.8, 3.6, 3.1, and 2.8 Mbps of capacity at N=250.

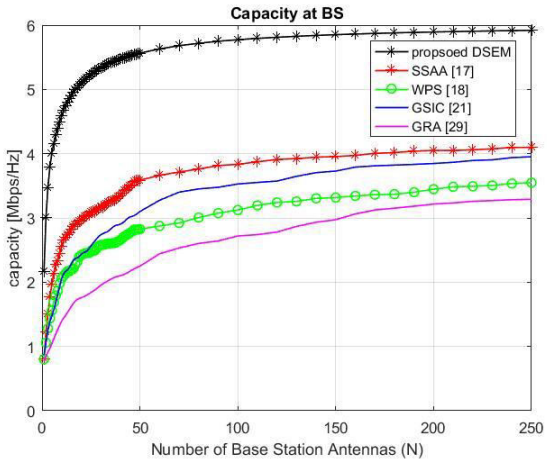

Figure-8. BS capacity performance estimation.

5. CONCLUSIONS

This work is implemented with the DSEM channel estimation method for Massive-MIMO-NOMA systems, in which channels can be divided based on sparsity. Here, the DSEM scheme divides the channel into expectation and maximization vectors based on antenna diversity. Further, time sample and frequency band base dual channel analysis are performed to maintain the synchronization in the receiver. The simulation results revealed that the proposed DSEM-based Massive-MIMO-NOMA systems outperformed as compared to conventional approaches concerning UE-capacity, BS-capacity, UL-SE, and DL-SE metrics. This work can be extended with advanced deep learning models for better SE improvement, as well as improvement of energy efficiency.

REFERENCES

[1] Senel K., Cheng H. V., Björnson E. and Larsson E. G. 2019. What role can NOMA play in massive MIMO? IEEE Journal of Selected Topics in Signal Processing. 13(3): 597-611.

[2] Dai Linglong, *et al*. 2018. Hybrid precoding-based millimeter-wave massive MIMO-NOMA with simultaneous wireless information and power transfer. IEEE Journal on Selected Areas in Communications. 37.1: 131-141.

[3] Zeng Ming, *et al*. 2019. Securing downlink massive MIMO-NOMA networks with artificial noise. IEEE Journal of Selected Topics in Signal Processing. 13.3: 685-699.

[4] Liu Lei, *et al*. 2018. Gaussian message passing for overloaded massive MIMO-NOMA. IEEE Transactions on Wireless Communications. 18.1: 210-226.

[5] de Sena A. S., Lima F. R. M., da Costa D. B., Ding, Z., Nardelli P. H., Dias U. S. and Papadias C. B. 2020. Massive MIMO-NOMA networks with imperfect SIC: Design and fairness enhancement. IEEE Transactions on Wireless Communications. 19(9): 6100-6115.

[6] Rezaei, Fatemeh, *et al*. 2020. Underlaid spectrum sharing for cell-free massive MIMO-NOMA. IEEE Communications Letters. 24.4: 907-911.

[7] Rezaei F., Tellambura C., Tadaion A. A. and Heidarpour A. R. 2020. Rate analysis of cell-free massive MIMO-NOMA with three linear precoders. IEEE Transactions on Communications. 68(6): 3480-3494.

[8] Al-Hussaibi, Walid A. and Falah H. Ali. 2019. Efficient user clustering, receive antenna selection, and power allocation algorithms for massive MIMO-NOMA systems. IEEE Access. 7: 31865-31882.

[9] Nguyen, The Khai, Ha H. Nguyen and Hoang Duong Tuan. 2020. Max-min QoS power control in generalized cell-free massive MIMO-NOMA with optimal backhaul combining. IEEE Transactions on Vehicular Technology. 69.10: 10949-10964.

[10] de Sena, Arthur Sousa, *et al*. 2021. IRS-assisted massive MIMO-NOMA networks: Exploiting wave polarization. IEEE Transactions on Wireless Communications. 20.11: 7166-7183.

[11] de Sena, Arthur Sousa, *et al*. 2019. Massive MIMO-NOMA networks with multi-polarized antennas. IEEE Transactions on Wireless Communications. 18.12: 5630-5642.

[12] Wang, Zhongyu, *et al*. 2021. Energy-efficient resource allocation in massive MIMO-NOMA networks with wireless power transfer: A distributed ADMM approach. IEEE Internet of Things Journal. 8.18: 14232-14247.

[13] Zhang Yao, *et al*. 2019. Spectral efficiency maximization for uplink cell-free massive MIMO-NOMA networks. 2019 IEEE International Conference on Communications Workshops (ICC Workshops). IEEE.

[14] Gao Z., Liu A., Han C. and Liang X. 2021. Sum rate maximization of massive MIMO NOMA in LEO satellite communication system. IEEE Wireless Communications Letters. 10(8): 1667-1671.

[15] Kaur Jaipreet and Maninder Lal Singh. 2019. User assisted cooperative relaying in beamspace massive MIMO NOMA based systems for millimeter wave communications. China Communications. 16.6: 103-113.

[16] Cao Yanmei, *et al*. 2021. A deep Q-network based-resource allocation scheme for massive MIMO-NOMA. IEEE Communications Letters. 25.5: 1544-1548.

[17] de Sena A. S., da Costa D. B., Ding Z., Nardelli P. H., Dias U. S. and Papadias C. B. 2019. Massive MIMO-NOMA networks with successive sub-array activation. IEEE Transactions on Wireless Communications. 19(3): 1622-1635.

[18] Ahmad Muneeb and Soo Young Shin. 2022. Massive MIMO NOMA with wavelet pulse shaping to minimize undesired channel interference. ICT Express.

[19] Sur Samarendra Nath, *et al*. 2022. Hybrid Precoding Algorithm for Millimeter-Wave Massive MIMO-NOMA Systems. Electronics. 11.14: 2198.

[20] Salehi Pouria, Naser Parhizgar and Farshad Pesaran. 2021. A New Cooperative and Distributed Antenna Structure in Massive MIMO-NOMA Based on mmWave Transmission Scheme. Wireless Communications and Mobile Computing 2021.

[21] Hu, Cheng, Hong Wang, and Rongfang Song. 2021. Group Successive Interference Cancellation Assisted Semi-Blind Channel Estimation in Multi-Cell Massive MIMO-NOMA Systems. IEEE Communications Letters. 25.9: 3085-3089.

[22] Alnajjar Khawla A. and Mohamed El-Tarhuni. 2019. A CV-BLAST spread spectrum massive MIMO NOMA scheme for 5G systems with channel imperfections. Physical Communication. 35: 100720.

[23] Li Yikai and Gayan Amarasuriya Aruma Baduge. 2020. Relay-Aided Downlink Massive MIMO NOMA with Estimated CSI. IEEE Transactions on Vehicular Technology. 70.3: 2258-2271.

[24] Liu Penglu, *et al*. 2020. Multi-beam NOMA for millimeter-wave massive MIMO with lens antenna array. IEEE Transactions on Vehicular Technology. 69.10: 11570-11583.

[25] Amirifar Zahra and Jamshid Abouei. 2022. The dynamic power allocation to maximize the achievable sum rate for massive MIMO-NOMA systems. IET Communications.

[26] Jawarneh Ahlam, Michel Kadoch and Zaid Albataineh. 2022. Decoupling energy efficient approach for hybrid precoding-based mmWave massive MIMO-NOMA with SWIPT. IEEE Access. 10: 28868-28884.

[27] Jiang Jing, Ming Lei and Huanhuan Hou. 2019. Downlink multiuser hybrid beamforming for MmWave massive MIMO-NOMA system with imperfect CSI. International Journal of Antennas and Propagation 2019.

[28] Simon E. P., Farah J., Laly P. and Delbarre G. 2021. A Gradual Resource Allocation Technique for Massive MIMO-NOMA. IEEE Antennas and Wireless Propagation Letters. 21(3): 476-480.

[29] Li S., Wan Z., Jin L. and Du J. 2019. Energy harvesting maximizing for millimeter-wave massive MIMO-NOMA. Electronics. 9(1): 32.

[30] Wang Shiguo, *et al*. 2021. Clustering and power optimization in mmWave massive MIMO-NOMA systems. Physical Communication. 49: 101469.